Materials Transactions, Vol. 61, No. 9 (2020) pp. 1717 to 1726

Mixing Entropy of Exact Equiatomic High-Entropy Alloys Formed into a Single Phase

Akira Takeuchi*

Graduate School of Engineering, Tohoku University, Sendai 980-8579, Japan

Exact equiatomic high-entropy alloys (EE-HEAs) comprising N elements ($N \geq 5$) formed into a single phase with either bcc, fcc or hcp structure were investigated based on sub-regular solution model. The analysis was performed by utilizing relationships among Gibbs energy (G), enthalpy (H), entropy (S), absolute temperature (T) and pressure (P), $G = H - TS$ and $S = -(\partial G/\partial T)_P$, for representative EE-HEAs, such as bcc-MoNbTaVW, fcc-CoCrFeMnNi and hcp-EE-HEAs comprising heavy lanthanides with and without Y. Mixing entropy (S^{mix}) was evaluated as the sum of excess entropy (S^{excess}) and ideal entropy (S^{ideal}), the latter of which is equivalent to configuration entropy (S^{config}). Calculation tools contained commercial software (Thermo-Calc 2020a) using a database for HEAs (TCHEA4) mainly for the bcc- and fcc-EE-HEAs and that for solid solutions (SSOL5) for the hcp-EE-HEAs. The analysis revealed that the bcc-MoNbTaVW and NbTaTiVW HEAs exhibited the greatest decrease in S^{mix} normalized with gas constant (R) down to approximately 87% of $S^{\mathrm{ideal}}/R = \ln N$ due to a positive T dependence of interaction parameter, $\Omega_{\mathrm{i-j}}(T)$, of i-j atomic pairs in mixing enthalpy (H^{mix}). In contrast, S^{mix}/R of the fcc-CoCrFeMnNi HEA was approximately 9% greater than $\ln N$. The hcp-EE-HEAs from a class of athermal solutions behaved as ideal solutions in practice. The results revealed that a relationship of $S^{\mathrm{mix}}/R = \ln N$ does not always hold in EE-HEAs. [doi:10.2320/matertrans.MT-M2020141]

(Received April 30, 2020; Accepted June 9, 2020; Published July 17, 2020)

Keywords: *high-entropy alloy, sub-regular solution model, interaction parameter, mixing entropy, excess entropy*

1. Introduction

Recently, increasing scientific attention has drawn to high-entropy alloys (HEAs)[1–3] as advanced metallic materials because of their unique properties. The terminology of HEAs originates from a large magnitude of entropy (S) when alloying or mixing in a multi-component system with equiatomic or near equiatomic ranging 5 to 35 at%. The large magnitude of S contributes to decreasing Gibbs energy (G) of the system of HEAs due to the thermodynamic formula of $G = H - TS$ where H and T are enthalpy and absolute temperature, respectively, leading to stabilizing G of a solid solution. The latest definitions of HEAs have allowed us to contain multiple phases including intermetallic compounds as well as a single phase. However, HEAs formed into a single phase is of great importance to analyze the fundamental features of HEAs.

Under the circumstances, the present paper describes thermodynamic analysis and calculations of exact equiatomic (EE) HEAs[4,5] formed into a single phase for their mixing entropy (S^{mix}) by focusing on excess entropy (S^{excess}).[6] Specifically, thermodynamic relationships among G, H, S, T and pressure (P), $G = H - TS$ and $S = -(\partial G/\partial T)_P$, were utilized to evaluate S^{excess}. In analyzing, types of solid solutions were considered to characterize the thermodynamic features of EE-HEAs for a set of mixing enthalpy (H^{mix}) and S^{mix}. Since EE-HEAs, as well as conventional HEAs, are a class of solid solutions, they should be classified into either

(1) ideal solution: $(H^{\mathrm{mix}}, S^{\mathrm{mix}}) = (0, S^{\mathrm{ideal}})$,
(2) athermal solution: $(H^{\mathrm{mix}}, S^{\mathrm{mix}}) = (0, \neq S^{\mathrm{ideal}})$,
(3) regular solution: $(H^{\mathrm{mix}}, S^{\mathrm{mix}}) = (\neq 0, S^{\mathrm{ideal}})$, or
(4) real solution: $(H^{\mathrm{mix}}, S^{\mathrm{mix}}) = (\neq 0, \neq S^{\mathrm{ideal}})$.

Here, $S^{\mathrm{mix}} = S^{\mathrm{ideal}}$ holds for ideal and regular solutions where S^{mix} exactly corresponds to configuration entropy (S^{config}) described below. Features of the regular solution are that S is supposed to be composed of only a term S^{ideal} and that the other excess terms regarding S (S^{excess}), even if they exist, deviated from an ideal state are included in H^{mix} as an excess G (G^{excess}) in alloying or mixing. This inclusion can be dealt with a sub-regular solution model with an interaction parameter, $\Omega_{\mathrm{i-j}}(\mathrm{x_i},\mathrm{x_j},T)$, of the i-j atomic pairs as functions of the contents of $\mathrm{x_i}$ and $\mathrm{x_j}$ ($0 \leq \mathrm{x_i}, \mathrm{x_j} \leq 1$) and T. However, this inclusion is never considered with a sub-regular solution model with a constant interaction parameter ($\Omega_{\mathrm{i-j}}$). In reality, T dependence of H^{mix} and S^{excess} cannot be recognized even with a sub-regular solution model at a glance without performing thermodynamic calculations in practice. This can simply be exemplified by a case that an additional bT term in H affects G by a formula of $G = H - TS$. Specifically, an additional bT term with b being a positive value that resulted from H as $(H + bT) - TS$ in the sub-regular solution model can also be interpreted as $H - T(S - b)$ as an additional term of S. This suggests[6] that the temperature dependence of H^{mix}, bT, can be regarded as S^{excess} with the ability to reduce its magnitude by b when b is a positive value. This two-aspects of the bT term between H and S motivated the present study to evaluate S^{mix} precisely based on the sub-regular solution model.

The present study also submits a problem with mixture usage of S^{mix} and S^{ideal}. By assuming HEAs as regular solutions, S^{mix} is often described incorrectly in many literature as eqs. (1) with a content of the i-th element ($\mathrm{x_i}$) and resultant $\mathrm{x_i} = N^{-1}$ in EE-EHAs where R is gas constant.

$$S^{\mathrm{mix}} = -R\sum_{i=1}^{N} \mathrm{x_i} \ln \mathrm{x_i} = R \ln N \tag{1}$$

Originally, eqs. (1) should be described for S^{config} that exactly corresponds to S^{ideal} as eqs. (2). Relationships in eqs. (2) always hold regardless of the four types of solid solutions. In strong contrast, eqs. (1) can be valid only for the alloys of interest are regarded as ideal and regular solutions.

*Corresponding author, E-mail: akira.takeuchi.a8@tohoku.ac.jp

$$S^{\text{config}} = S^{\text{ideal}} = -R\sum_{i=1}^{N} x_i \ln x_i = R \ln N \quad (2)$$

In other words, eqs. (1) does not necessarily valid for athermal and real solutions with a relationship $S^{\text{mix}} \neq S^{\text{ideal}}$. Thus, it is worth analyzing S^{mix} for EE-HEAs to characterize thermodynamic nature.

Based on the above consideration, the present study regards S^{mix} of experimentally observed EE-HEAs formed into a single-phase (as an arbitral α-phase: $\alpha =$ bcc, fcc or hcp) could be described as eq. (3) by considering additional term of S^{excess}.

$$S^{\text{mix}} = S^{\text{config}} + S^{\text{excess}} \quad (3)$$

Besides, allotropic entropy ($\Delta S^{\text{allotropic},\beta\text{-}\neq\alpha\text{-phase}}$) due to the difference in the phase of interest of constituent elements might be necessary to take into account in evaluating S^{mix}. However, preliminary investigation revealed that $\Delta S^{\text{allotropic},\beta\text{-}\neq\alpha\text{-phase}}$ affects in the form of linear function and shifts S^{mix} by the content of the i-th element of the alloys in a composition–G diagram by the value of $x_i \cdot \Delta S^{\text{allotropic},\beta\text{-}\neq\alpha\text{-phase}}$ for each content. In reality, $\Delta S^{\text{allotropic},\beta\text{-}\neq\alpha\text{-phase}}$ term works only when the phase of interest of alloy, α-phase that is acquired from experiments, differs from that of the constituent element, β-phase $\neq$ α-phase. In other words, $\Delta S^{\text{allotropic},\beta\text{-}\neq\alpha\text{-phase}}$ can be ignored when the phases of the alloy and constituent elements are the same at given T and P. Thus, $\Delta S^{\text{allotropic},\beta\text{-}\neq\alpha\text{-phase}}$ does not affect the formulae of eq. (3) essentially.

The present paper aims to examine whether the formula, $S^{\text{mix}} = R \ln N$, holds for EE-HEAs actually by performing thermodynamic evaluations and to clarify the contribution of S^{excess} to S^{mix} in forming in N-component EE-HEAs formed into a single phase.

2. Methods

2.1 Thermodynamic analysis

We dealt with a set of thermodynamic quantities of G, H, and S of an N-element alloy ($N \geq 5$) with x_i, which satisfies $\sum_{i=1}^{N} x_i = 1$. Only a single phase of alloys under a constant P was considered to simplify the subsequent analysis. In the actual analysis, molar thermodynamic quantities were considered, such as, molar G, H, and S (G, H, and S per one mole of atoms) by giving a symbol (m) at subscript of each G, H, and S below. In short, molar mixing entropy (S_m^{mix}) was analyzed as a function of T in a process of evaluating molar mixing Gibbs energy (G_m^{mix}) with a single phase of the EE-HEAs as a function of T. In practice, the present study defined that G_m^{mix} is a quantity with values of zero at the pure constituent elements as eq. (4).

$$G_m^{\text{mix}} = G_m^{\alpha} - \sum_{i=1}^{N} x_i {}^0G_m^{\alpha\text{-i}} \quad (4)$$

Here, ${}^0G_m^{\alpha\text{-i}}$ is a molar G of an α-phase ($\alpha =$ bcc, fcc or hcp) of the i-th element at a given T and P where superscript zero indicates the pure state of the element. The α-phase was set to be the same as that of HEA experimentally observed. When the α-phase did not correspond to a standard element reference (SER) that was defined by CALPHAD (CALculation of PHAase Diagrams) scheme of the i-th element that resulted from the stable crystallographic phase at a given T and P, additional G term of allotropic transformation ($\Delta G^{\text{allotropic}}$) took place, but the present study did not deal with $\Delta G^{\text{allotropic}}$ furtherly as described in the former Section. Besides, there is another definition of SER in Thermo-Calc software[7] that stands for selected element reference. The SER's from CALPHAD and Thermo-Calc software are equivalent in practice.

2.2 Alloys

Among 100 or more HEAs[2,3] found to date, the EE-HEAs that are formed into a single-phase either a simple crystallographic structure of bcc, fcc, or hcp phase as solid solutions were considered for evaluations. In reality, the EE-HEAs were acquired form a book[3] and their original literature by limiting their preparation methods of either arc-melting or induction melting, and subsequent annealing in need. These production methods matched the concept of HEAs that are thermodynamically stable solid solutions due to large S value, reducing G of systems due to $G = H - TS$. The actual alloys investigated were 18 bcc-EE-HEAs consisting of HfMoNbTiZr,[8] MoNbTaVW,[9,10] MoNbTaTiVW,[11] CrMoNbReTaVW[12] and others,[13–21] 9 fcc-EE-HEAs of CoCrFeMnNi[22–24] and others,[25–32] and 4 hcp-EE-HEAs of DyGdHoTbY,[33] DyGdLuTbY and DyGdLuTbTm[34] and GdHoLaTbY.[35]

2.3 Interaction parameter, $\Omega_{i-j}(T)$, of H_m^{mix} in a formula of sub-regular solution model and relationships between G_m^{mix} and G_m^{excess}

First, G_m^{mix} of EE-HEAs were calculated with Thermo-Calc as a function of T. Then, G_m^{mix} was fitted with coefficients a, b, c as described in eqs. (5).

$$\begin{aligned} G_m^{\text{mix}} &= a + bT + cT \ln T \\ &= a + (b + c \ln T)T \end{aligned} \quad (5)$$

It might be necessary to consider the succeeding terms to $cT \ln T$ at the first line on the right side of eqs. (5), such as, by adding T^n ($1 < n \leq 4$ or 7) and T^{-m}, ($m = 1$ or 9) as can be seen in unary SGTE (Scientific Group Thermodata Europe) database.[36] However, preliminary investigation revealed that most of the alloys including the EE-HEAs investigated in the present study can be described G_m^{mix} as well as G_m^{α} in eq. (4) up to the three terms as the first line on the right side of eqs. (5). In case of requiring further additional terms, see details in the Appendix.

On the other hand, in a framework of a sub-regular solution model, H_m^{mix} can be described with $\Omega_{i-j}(T)$ as eqs. (6) and (7) when the fitting G_m^{mix} was thoroughly made up to the $T \ln T$ term.

$$\begin{aligned} H_m^{\text{mix}} &= \sum_{j\neq i}^{N}\sum_{i=1}^{N} \Omega_{i\text{-}j}(T) x_i x_j \\ &= 4\sum_{j\neq i}^{N}\sum_{i=1}^{N}\left\{\sum_{v=0}^{v} L_{i\text{-}j}^{(v\text{-th})}(T)(x_i - x_j)^v\right\} x_i x_j \end{aligned} \quad (6)$$

$$L_{i\text{-}j}^{(v\text{-th})}(T) = a_{i\text{-}j}^{(v\text{-th})} + b_{i\text{-}j}^{(v\text{-th})} T + c_{i\text{-}j}^{(v\text{-th})} T \ln T \quad (7)$$

Here, a part of the right side of eqs. (6) described in a formula of Redlich-Kister (R-K) polynomial functions of $(x_i - x_j)^v$ can be expressed as eqs. (8) for EE-HEAs with $v = 0$ due to a relationship of $x_i = x_j = N^{-1}$ for every i-j atomic pair.

$$\begin{aligned}\sum_{j\neq i}^{N}\sum_{i=1}^{N}\left\{\sum_{v} L_{ij}^{(v)}(T)(x_i - x_i)^v\right\}x_i x_i &= \sum_{j\neq i}^{N}\sum_{i=1}^{N}\left\{\sum_{v} L_{ij}^{(v)}(T)\left(\frac{1}{N}-\frac{1}{N}\right)^v\right\}\frac{1}{N^2}\\ &= \frac{1}{N^2}\sum_{j\neq i}^{N}\sum_{i=1}^{N}\left\{\sum_{v} L_{ij}^{(0)}(T)\right\}\end{aligned} \tag{8}$$

Eventually, eqs. (6) and (7) can be simplified as eqs. (9).

$$\begin{aligned}H_{m,\,EE\text{-}HEA}^{mix} &= 4N^{-2}\sum_{j\neq i}^{N}\sum_{i=1}^{N}(a_{i\text{-}j}^{(0)} + b_{i\text{-}j}^{(0)}T + c_{i\text{-}j}^{(0)}T\ln T)\\ &= a^{(0)} + b^{(0)}T + c^{(0)}T\ln T\\ &= L_{EE\text{-}HEA}^{(0)}(T)\end{aligned} \tag{9}$$

Here, $\Omega_{i-j}(T)$ in eqs. (6) originated from the sub-regular solution model, which enables us to deal with asymmetric composition dependence of H_m^{mix} against equiatomic composition ($x_A = x_B = 0.5$) in an A–B binary system due to the presence of v from odd numbers. On the other hand, coefficient four on the right side of eqs. (6) is a modifier to $x_i x_j$ term so that $L_{i\text{-}j}^{(v\text{-th})}(T)$ corresponds to the actual value of $L_{i\text{-}j}^{(v\text{-th})}(T)$ at $x_i = x_j = 0.5$ in each binary system. A significant feature of EE-HEAs is that equiatomicity ($x_i = x_j$) holds for all atomic pairs, which greatly reduced the necessary terms to be considered to only one set of coefficients of the 0-th order $(a^{(0)}, b^{(0)}, c^{(0)}, \ldots)$ of $L_{EE\text{-}HEA}^{(0)}(T)$ in eqs. (9) due to $x_i = x_j$ in eqs. (6). This feature allows us to use a conventional regular solution model in practice as the 0-th order approximation of the sub-regular solution model at $x_i = x_j = N^{-1}$.

Next, we considered deriving the formula of the sub-regular solution model from eqs. (5). According to the sub-regular as well as the regular solution model, which defines S as $S_m^{config} = S_m^{ideal}$, one can rewrite eqs. (5) as eqs. (10) for EE-HEAs where S-RSM stands for the sub-regular solution model. In reality, the coefficients (a, b and c) without superscript (0) at the first line in eqs. (9) originated from a conventional description by eqs. (5) and those with superscript (0) at the second and third lines in eqs. (9) resulted from the 0-th order approximation of the S-RSM. The coefficients (a, b and c) with and without superscript (0) are equivalent to each other for EE-HEAs.

$$\begin{aligned}G_m^{mix} &= \{a + (b + c\ln T + S_m^{ideal})T\} - TS_m^{ideal}\\ &= \{a^{(0)} + (b^{(0)} + c^{(0)}\ln T + S_m^{ideal})T\} - TS_m^{ideal}\\ &= \{a^{(0)} + (b^{(0)} + c^{(0)}\ln T + R\ln N)T\} - TS_m^{ideal}\\ &= H_m^{mix\ (S\text{-}RSM)} - TS_m^{ideal}\\ &= G_m^{excess\ (S\text{-}RSM)} - TS_m^{ideal}\end{aligned} \tag{10}$$

At the first line on the right side of eqs. (10), a term of $-TS_m^{ideal}$ was intentionally added at the last term, which was compensated for by adding TS_m^{ideal} in the brace at the second term on the first line. Besides, $x_i = x_j$ for EE-HEAs made it possible to consider $v = 0$-th terms only described in eq. (7) and at the second and third lines of eqs. (10). The fourth line on the right side of eqs. (10) is the conventional description of the sub-regular solution model where mixing enthalpy is intentionally described as $H_m^{mix\ (S\text{-}RSM)}$. Note that a term $RT\ln N$ is added at the third line in eqs. (10) as $H_m^{mix\ (S\text{-}RSM)}$, which differs from $H_{m,\,EE\text{-}HEA}^{mix} = a^{(0)} + b^{(0)}T + c^{(0)}T\ln T$ where $RT\ln N$ is absent in eqs. (9). This was due to the two-aspect of the bT term between H and S in the sub-regular solution model as described in Section 1. The $RT\ln N$ term originates from S^{config}, which is equivalent to S^{ideal} from eqs. (2), and thus, the term $H_m^{mix\ (S\text{-}RSM)}$ containing S^{ideal} unconsciously in its formulation can be rewritten as G consisting of H and S instead of H solely. Consequently, the fourth line of eqs. (10) can be rewritten as the last line by regarding $H_m^{mix\ (S\text{-}RSM)} = a^{(0)} + (b^{(0)} + c^{(0)}\ln T + R\ln N)T$ for EE-HEAs as $G_m^{excess(S\text{-}RSM)}$. The significance of the appearance of $G_m^{excess(S\text{-}RSM)}$ in eqs. (10) will be explained in the next paragraph.

In contrast to eqs. (10), the present study provides another formula for describing G_m^{mix} as shown in eqs. (11) with keeping the relationships of $G = H - TS$ and $S = -(\partial G/\partial T)_P$.

$$\begin{aligned}G_m^{mix} &= a + bT + cT\ln T\\ &= (a^{(0)} - c^{(0)}T) - \{-b^{(0)} - c^{(0)}(\ln T + 1)\}T\\ &= (a^{(0)} - c^{(0)}T) - \{-b^{(0)} - c^{(0)}(\ln T + 1) - R\ln N\}T\\ &\quad - TS_m^{ideal}\\ &= H_m^{excess} - TS_m^{excess} - TS_m^{ideal}\\ &= H_m^{excess} - TS_m^{mix}(= G_m^{excess(S\text{-}RSM)} - TS_m^{ideal}\\ &= H_m^{excess(S\text{-}RSM)} - TS_m^{ideal})\end{aligned} \tag{11}$$

Note that mixing enthalpy at the fourth and fifth lines in eqs. (11) is intentionally expressed as H_m^{excess} to distinguish it from $H_m^{mix\ (S\text{-}RSM)}$ in eqs. (10), and thus, $H_m^{excess} = a^{(0)} - c^{(0)}T$ at the last line in eqs. (11) does not agree with $H_m^{mix\ (S\text{-}RSM)} = \{a^{(0)} + (b^{(0)} + c^{(0)}\ln T + R\ln N)T\}$ for EE-HEAs in eqs. (10). This difference again indicated the two-aspect of the bT term between H and S in sub-regular solution model as described in Section 1 in that only $= a^{(0)} - c^{(0)}T$ from H_m^{excess} should be considered as H in reality instead of $\{a^{(0)} + (b^{(0)} + c^{(0)}\ln T + R\ln N)T\}$ from $H_m^{mix\ (S\text{-}RSM)}$ in frameworks of thermodynamic quantities: $G = H - TS$ and $S = -(\partial G/\partial T)_P$. In short, the two-aspect allows us to describe $H_m^{mix\ (S\text{-}RSM)}$ in eqs. (9) from H_m^{excess} in eqs. (11) by converting TS_m^{excess} as an H term as shown at the fourth line in eqs. (11). Hence, neither $H_m^{excess} = a^{(0)} - c^{(0)}T$ nor $S_m^{excess} = \{-b^{(0)} - c^{(0)}(\ln T + 1)\}$ for EE-HEAs in eqs. (11) correlated with $G_m^{excess\ (S\text{-}RSM)} = \{a^{(0)} + (b^{(0)} + c^{(0)}\ln T + R\ln N)T\}$ for EE-HEAs in eqs. (10) in that the former (H_m^{excess} and S_m^{excess}) was from the thermodynamic excess quantities investigated in the present study and the latter ($G_m^{excess\ (S\text{-}RSM)}$) was due to the sub-regular solution model. Further attention should be paid to that the last line of eqs. (10), $G_m^{mix} = G_m^{excess(S\text{-}RSM)} - TS_m^{ideal}$, was also derived in eqs. (11) by considering $S_m^{excess} = -b^{(0)} - c^{(0)}(\ln T + 1) - R\ln N$ for EE-HEAs.

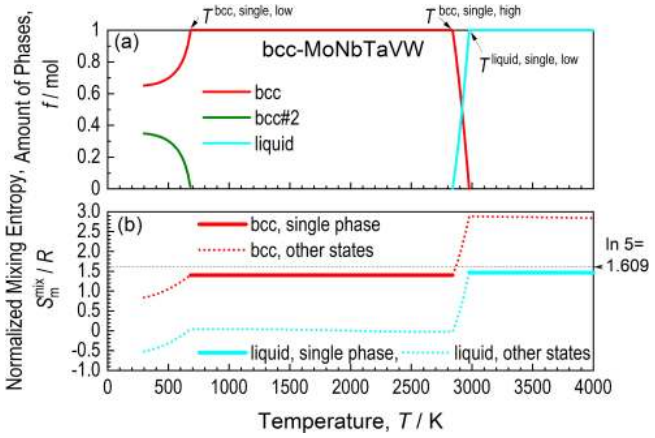

Fig. 1 (a) Stable phases and their amounts in the unit of one mole of the bcc-MoNbTaVW EE-HEA calculated with Thermo-calc 2020a and the TCHEA4 database. A single bcc phase was stable at a wide temperature range of 682.9 ~ 2839.3 K ($T^{bcc, single, low} \sim T^{bcc, single, high}$), whereas a single liquid phase was stable at $T \geq 2976.5$ K ($T^{liquid, single, low}$). (b) The values of S_m^{mix}/R of the bcc-MoNbTaVW EE-HEA at bcc and liquid single phases (solid thick curves), respectively, and those at other states (dotted curves).

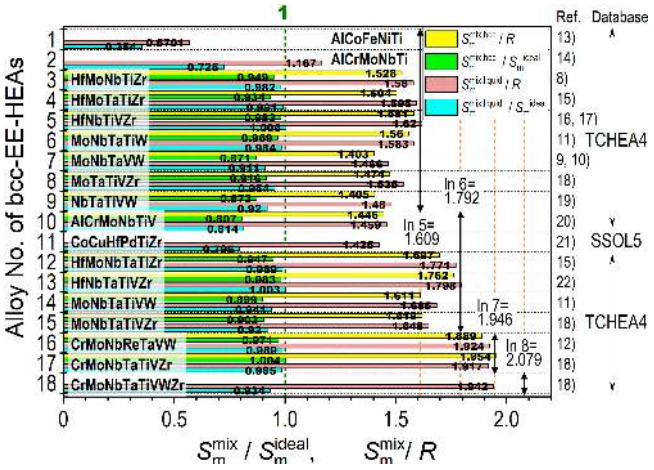

Fig. 2 Values of S_m^{mix}/S_m^{ideal} and S_m^{mix}/R of bcc-EE-HEAs in single bcc calculated with Thermo-calc at 1600 K and liquid phases at 4000 K, together with original references and database for calculations. Each horizontal columns have four bars at the maximum as shown in the explanatory notes. Bars of bcc single phase of Nos. 1, 2, 11 and 18 were absent, since the single bcc phase was not achieved from calculations. Temperature ranges of a single bcc and liquid phase are supplementary shown in Fig. 5.

3. Results and Discussion

3.1 bcc-EE-HEAs

The analysis revealed that 14 in 18 alloys[8–21] exhibited a single bcc phase from calculations with Thermo-Calc. Specifically, S_m^{mix} was computed for 14 alloys for both bcc and liquid phases whereas S_m^{mix} of liquid phase only was calculated for the other 4 alloys (AlCoFeNiTi, AlCrMoNbTi, CoCuHfPdTiZr, and CrMoNbTaTiVWZr). As a set of examples, amounts of phases, and S_m^{mix}/R of the bcc and liquid phases of the bcc-MoNbTaVW EE-HEA are shown in Fig. 1. Figure 1(a) shows that a single bcc phase was stable at a wide temperature range of 682.9 ~ 2839.3 K ($T^{bcc, single, low} \sim T^{bcc, single, high}$), whereas a single liquid phase was stable at $T \geq 2976.5$ K ($T^{liquid, single, low}$). At a range of T lower than 682.9 K, this alloy exhibited dual bcc-phase of bcc+bcc#2 from calculation results. Figure 1(b) demonstrates S_m^{mix}/R of the single bcc and liquid phases drawn with thick solid curves, accompanied by those of the other states with dotted curves. Each S_m^{mix}/R of a single bcc and liquid phase is almost constant, which are slightly smaller than $\ln 5 \sim 1.609$, whereas S_m^{mix}/R of the single liquid phase is slightly larger than that of the single bcc phase. Figure 1(b) indicates that bcc-MoNbTaVW EE-HEA in both bcc and liquid single-phase dose not possess $S_m^{mix}/R = \ln 5$. Figure 1(b) artificially demonstrates the change in S_m^{mix}/R due to the phase transitions: phase separation at $T < 682.9$ K ($T^{bcc, single, low}$) and a mixture of bcc and liquid phases at $T = 2839.3 \sim 2976.5$ K ($T^{bcc, single, high} \sim T^{liquid, single, low}$). The latter case corresponds to the increase/decrease in S_m^{mix}/R due to the melt/solidification of the alloy. The values shown in dotted curves were calculated artificially, but the values of S_m^{mix}/R were in principle valid only for the calculation results for a single-phase drawn in thick solid curves.

Calculation results of the S_m^{mix} and their ratio to S_m^{ideal} of the all alloys including the bcc-MoNbTaVW EE-HEA are depicted in Fig. 2. In Fig. 2, the values of S_m^{mix}/R were calculated for single bcc and liquid phases at 1600 and 4000 K, respectively. These temperatures were determined by the calculation results that all the 14 alloys in bcc-phase and all the 18 alloys in liquid phase exhibited a single phase at these temperatures and that S_m^{mix}/R were almost unchanged at each temperature range forming a single phase as depicted in Fig. 1(b). Figure 2 shows that the values of the ratio, S_m^{mix}/S_m^{ideal}, of bcc phase (given at the second horizontal bar in each column numbered and drawn in a light-green bar in online version) are approximately in the range of 0.9 to 1, excepting for alloys with Nos. 7, 9 and 10 that tended to exhibit lower ratios than $S_m^{mix}/S_m^{ideal} \sim 0.9$. Only the CrMoNbTaTiVZr EE-HEA (No. 17) of a single bcc phase exhibits slightly greater than $S_m^{mix}/S_m^{ideal} = 1$. As for the ratios of S_m^{mix}/S_m^{ideal} of liquid phase (given at the fourth bar in each column numbered and light-blue in green bar in the online version), alloys with No. 1, 2, 10 and 11 had a tendency exhibiting lower S_m^{mix}/S_m^{ideal} than approximately 0.8. Here, No. 11 may be excluded from this tendency, since SSOL5 database was used for calculating S_m^{mix}/R due to the inclusion of Pd that is out of the applicability of TCHEA4. Only the HfNbTiVZr EE-HEA (No. 5) and HfNbTaTiVZr EE-HEA (No. 13) of a single liquid phase exhibit slightly greater than $S_m^{mix}/S_m^{ideal} = 1$. As a whole, it is found that alloys with V and W simultaneously (Nos. 7 and 9) and with Al (Nos. 1, 2 and 10), in particular with atomic pairs of Al–Fe or Al–Ti, seemed to cause smaller S_m^{mix}/S_m^{ideal}. However, the effect of decreasing tendency of S_m^{mix}/S_m^{ideal} of alloys with V and W simultaneously (Nos. 7 and 9) was weakened in further multicomponent alloying with $N > 5$, which can be seen in the values of $S_m^{mix}/S_m^{ideal} \sim 0.9$ or more in alloys in Nos. 14, 16 and 18. The reason for decreasing in S_m^{mix}/R with the addition of V and W simultaneously in Nos. 7 and 9 and with Al–Fe or Al–Ti atomic pairs will be explained in Section 3.4.

3.2 fcc-EE-HEAs

The calculation results of the nine fcc-EE-HEAs are

Table 1 Values of S_m^{mix}/R of the fcc-EE-HEAs calculated with Thermo-Calc. Calculations were performed for a single fcc and liquid phase at 1300 and 4000 K, respectively, which are common for all alloys exhibiting a single phase.

No	Alloy	Ref	N	ln N	Phase	Temp. Range of Single Phase	S_m^{mix}/R	S_m^{mix}/S_m^{ideal}	Database
1	AuCuNiPdPt	[25]	5	1.609	fcc	893.3~1488.3	1.35703	0.843	SSOL5
					liquid	1555.0~	1.50270	0.934	
2	CoCrCuFeNi	[26]			mixed	—	—	—	TCHEA4
					liquid	1561.1~	1.61390	1.003	
3	CoCrFeMnNi	[22-24]			fcc	1105.2~1560.7	1.74988	1.087	
					liquid	1596.0~	1.55180	0.964	
4	CoCrFeNiTi	[27]			mixed	—	—	—	
					liquid	1402.7~	1.20345	0.748	
5	CoCuFeMnNi	[28]			fcc	1003.5~1429.8	1.61498	1.003	
					liquid	1541.3~	1.63236	1.014	
6	CoCuFeNiTi	[29]			mixed	—	—	—	
					liquid	1428.9~	1.09576	0.681	
7	CrCuFeMoNi	[30]			mixed	—	—	—	
					liquid	2218.0~	1.29762	0.806	
8	CuFeMnNiPt	[31]			fcc	1261.6~1383.5	1.47943	0.919	SSOL5
					liquid	1588.6~	1.46138	0.908	
9	CuIrNiPdPtRh	[32]	6	1.792	fcc	1279.5~1724.2	1.84865	1.032	
					liquid	1850.9~	1.69209	0.944	

summarized in Table 1 where these alloys were reported[22–32] as a single fcc-EE-HEAs through either arc-melting or induction melting and subsequent annealing in need. Of nine alloys, five alloys of AuCuNiPdPt, CoCrFeMnNi, CoCuFeMnNi, CuFeMnNiPt and CuIrNiPdPtRh with Nos. 1, 3, 5, 8 and 9, respectively, exhibited a single fcc phase from calculations with Thermo-Calc. Specifically, calculations were performed with TCHEA4 database for two alloys of CoCrFeMnNi and CoCuFeMnNi EE-HEAs (Nos. 3 and 5) whereas the other three alloys containing Pd, Pt, and Rh (Nos. 1, 8 and 9) were with SSOL5 database. The calculation results summarized in Table 1 show that the ratios of S_m^{mix}/S_m^{ideal} of fcc phase were in the range of approximately 0.85 (No. 1) to 1.09 (No. 3) whereas those of liquid phase was nearly 0.68 (No. 6) to 1.01 (No. 5). Here, it should be noted that the CoCrFeMnNi (No. 3), CoCuFeMnNi (No. 5) and CuIrNiPdPtRh (No. 9) in fcc phase as well as CoCrCuFeNi (No. 2) and CoCuFeMnNi (No. 5) in liquid phase exhibit greater $S_m^{mix}/S_m^{ideal} = 1$. The greatest value of the ratios of $S_m^{mix}/S_m^{ideal} = 1.087$ was calculated in the CoCrFeMnNi (No. 3) for its fcc phase. On the other hand, alloys containing Ti at a liquid phase appear to exhibit low $S_m^{mix}/S_m^{ideal} < 0.7$ as shown in alloys CoCrFeNiTi (No. 4) and CoCuFeNiTi (No. 6). Furthermore, the CrCuFeMoNi (No. 7) in a liquid phase also exhibit small $S_m^{mix}/S_m^{ideal} \sim 0.8$. The reason for these decreases in S_m^{mix}/R of alloys in liquid phases with Nos. 4, 6 and 7 containing Fe and Ni together and with Ti or Mo will be explained in Section 3.4.

3.3 hcp-EE-HEAs

The calculations performed for four hcp-EE-HEAs with SSOL5 database are summarized in Table 2. Table 2 revealed that the DyGdHoTbY, DyGdLuTbY and DyGdLuTbTm alloys were formed into a single hcp phase as experimental results.[33,34] On the other hand, the GdHoLaTbY exhibited a single bcc phase from calculations as a stable phase instead of the hcp phase from experiment.[35] The results clearly show that hcp-EE-HEAs possesses ideal $S_m^{mix}/S_m^{ideal} = 1$ in solid and liquid states. This coincidence is due to the chemical similarity between the constituents that are selected from heavy lanthanides mainly. The chemical similarity of Y to heavy lanthanides also contributes to the $S_m^{mix}/S_m^{ideal} = 1$. These results indicate that the hcp-EE-HEAs, which were classified into athermal solutions, behaved as ideal solutions in practice.

3.4 Temperature dependence of $\Omega_{i-j}(T)$ and its effect on S_m^{mix}/R

The calculation results as shown in Fig. 2 demonstrated that relatively large decrease in S_m^{mix}/R from $S_m^{ideal}/R = \ln N$ were observed in bcc-EE-HEAs with simultaneous inclusions of V and W bcc-EE-HEAs in a bcc phase (Nos. 7, 9 in Fig. 2) and Al-containing bcc-EE-HEAs in a liquid phase as well as bcc phases (Nos. 1, 2 and 10 in Fig. 2). In contrast, Table 1 declared that $S_m^{mix}/R > S_m^{ideal}/R = \ln N$ were observed in the CoCrFeMnNi and CoCuFeMnNi fcc-EE-HEAs (Nos. 3 and 5 in Table 1) in an fcc phase. This Sub-Section discloses the reason for these peculiar deviations of S_m^{mix}/R from $S_m^{ideal}/R = \ln N$.

Table 2 Values of S_m^{mix}/R of the hcp-EE-HEAs calculated with Thermo-Calc. Calculations were performed for a single hcp and liquid phase at 1600 and 4000 K, respectively, which are common for all alloys exhibiting a single phase. The GdHoLaTbY exhibited a single bcc phase instead of the hcp phase from calculation.

No	Alloy	Ref	N	ln N	Phase	Temp. Range of Single Phase	S_m^{mix}/R	S_m^{mix}/S_m^{ideal}	Database
1	DyGdHoTbY	33)	5	1.609	hcp	298.15~1649.0	1.60955	1.000	SSOL5
					liquid	1690.6~	1.60954	1.000	
2	DyGdLuTbY	34)			hcp	298.15~1712.6	1.60955	1.000	
					liquid	1724.0~	1.60954	1.000	
3	DyGdLuTbTm	34)			hcp	298.15~1719.9	1.60955	1.000	
					liquid	1732.0~	1.60954	1.000	
4	GdHoLaTbY	35)			(bcc)	(991.4~1607.7)	—	—	
					liquid	1622.0~	1.60954	1.000	

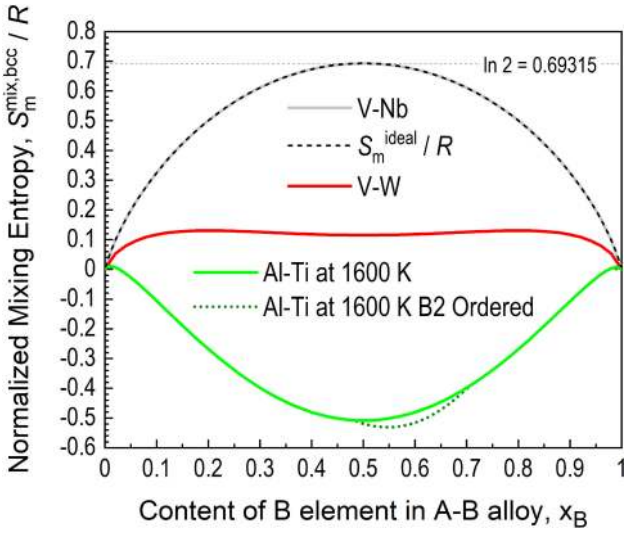

Fig. 3 S_m^{mix}/R of the V–Nb, V–W sub-binary systems, together with that of the Al–Ti binary system computed with Thermo-Calc at 1600 K and S_m^{ideal}/R for comparison. These values were calculated with Thermo-Calc using TCHEA4 database at a temperature range exhibiting a single bcc phase: 546.0–2192.3 K in V–Nb, 298.15–2632.9 K in V–W and 298.15–1666.8 K in Al–Ti sub-binary systems. The Al–Ti sub-binary system exhibited hcp and $L1_0$-AlTi as stable solid phases, and thus, bcc as well as B2 ordered and liquid phases only were intentionally selected for calculations. The G_m^{mix}/R of the V–Nb, V–W and Al–Ti sub-binary systems can be approximated up to $b^{(0)}T$ term.

First, the composition dependence of S_m^{mix}/R was preliminary calculated with Thermo-Calc at $T = 1600$ K for bcc phase for V–W and Al–Ti binary systems and V–Nb binary system for comparison. Figure 3 shows that S_m^{mix}/R at $x_B = 0.5$ of the V–W binary alloy is considerably smaller than that of V–Nb alloy that exactly exhibit S_m^{ideal}/R. Furthermore, the Al–Ti binary alloy exhibits negative S_m^{mix}/R smaller than -0.5 at a central composition range over equiatomicity. These different tendencies between V–Nb and other binary alloys were analyzed furtherly to explain with $\Omega_{i-j}(T)$ of an i–j atomic pair as a result of calculating G_m^{mix}. Here, B2 ordered phase was stable in Al–Ti binary system at 1600 K at $x_B \sim 0.5$–0.7 in Fig. 3, which was not investigated furtherly in the analysis of 0-th order approximation as shown later.

Table 3 Coefficients ($a^{(0)}$ and $b^{(0)}$) of the 0th order of the interaction parameter, $\Omega_{i-j}(T)$, of a single bcc phase of the V–Nb, V–W and Al–Ti binary alloy systems obtained by approximating G_m^{mix}. A single bcc phase was computed at a temperature range of 546.0–2192.3 K in V–Nb, 298.15–2632.9 K in V–W and 298.15–1666.8 K in Al–Ti sub-binary systems. The Al–Ti sub-binary system exhibited hcp and $L1_0$-AlTi as stable solid phases, and thus, bcc and liquid phases only were intentionally selected for calculations. The coefficients obtained by approximating G_m^{mix} up to T term with $\Omega_{i-j}(T) = 4\{a^{(0)} + (b^{(0)} + R\ln 2)T\}$ from the sub-regular solution model where S_m^{mix}/R was able to be computed as $-b^{(0)}/R$.

Alloy	$a^{(0)}$ / J·mol^{-1}	$(b^{(0)}+Rln2)$ / J·mol^{-1}·K^{-1}	$(-b^{(0)}/R)$ /·K^{-1}	S_m^{mix}/R in Fig. 3
V-Nb	2270	−0.00037	0.69319	0.693
V-W	−9729.3	4.8052	0.11518	0.115
Al-Ti (1600 K)	−39513.5	40.6051	−0.50842	−0.508

The above tendencies of T dependence of $\Omega_{i-j}(T)$ were investigated for the V–Nb, V–W and Al–Ti sub-binary systems summarized in Table 3. Table 3 shows that the values of S_m^{mix}/R of the V–Nb and V–W, which are previously shown in Fig. 3 as 0.69319 and 0.11518, respectively, was evaluated from Table 3 as $-b^{(0)}/R$. Similarly, S_m^{mix}/R of the exact equiatomic Al–Ti at 1600 K as a disordered bcc phase was calculated to be −0.50842, which is enough as fist approximation to $S_m^{mix}/R = -0.508$ in Fig. 3. The results of S_m^{mix}/R of the V–Nb and V–W indicate that S_m^{mix} cannot be S_m^{ideal} when H_m^{mix} has T dependence. In addition to the V–Nb sub-binary system, preliminary calculations, which are not shown in the current figures and tables, revealed that V–Mo, Nb–Ta, Mo–W sub-binary systems in a single bcc and liquid phase at 1600 and 4000 K, respectively, and V–Ta and Mo–Ta sub-binary system at 4000 K in a single liquid phase exhibited $S_m^{mix}/R \sim \ln 2$. As a whole, the minimum S_m^{mix}/R was observed in the V–W sub-binary system and the maximum $S_m^{mix}/R \sim \ln 2$ was in V–Nb and some other sub-binary systems in the MoNbTaVW EE-HEA. These tendencies explained approximately a 13% decrease in S_m^{mix}/R of a single bcc phase of the MoNbTaVW EE-HEA (No. 7) at

Table 4 Coefficients ($a^{(0)}$ and $b^{(0)}$) of the 0th order of the interaction parameter, $\Omega_{i-j}(T)$, of a single liquid phase of the of Ni–Ti, Fe–Ti and Mo–Ni binary alloy systems. A single liquid phase was obtained at a temperature range of 1583.7–4000 K in Ni–Ti, 1585.8–4000 K in Fe–Ti and 2018.3–4000 K in Mo–Ni sub-binary systems. The coefficients obtained by approximating G_m^{mix} up to T term with $\Omega_{i-j}(T) = 4\{a^{(0)} + (b^{(0)} + R\ln 2)T\}$ from the sub-regular solution model where S_m^{mix}/R was able to be computed as $-b^{(0)}/R$.

Alloy	$a^{(0)}$ / J·mol^{-1}	$(b^{(0)}+R\ln 2)$ /·K^{-1}	$S_m{}^{mix}/R = -b^{(0)}/R$ /·K^{-1}
Ni-Ti	−38427	8.7143	−0.3550
Fe-Ti	−19062	4.4609	0.1566
Mo-Ni	−11635	4.8821	0.1059

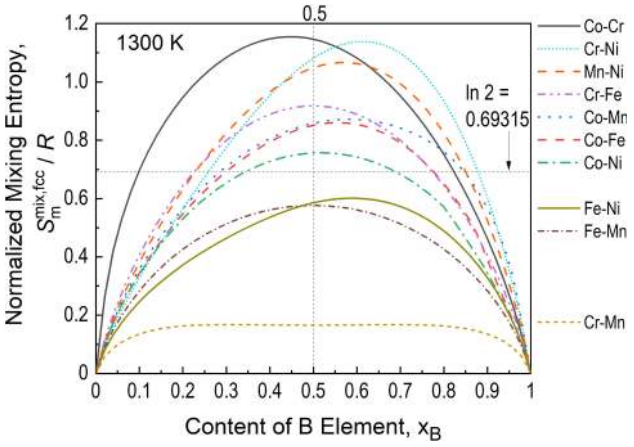

Fig. 4 S_m^{mix}/R of the sub-binary systems comprising CoCrFeMnNi fcc-EE-HEA calculated at 1300 K with Thermo-Calc using TCHEA4 database. The calculations were performed based on a sub-regular solution model, which can deal with asymmetry against $x_B = 0.5$.

1600 K as shown in Fig. 2. These tendencies also explained the CrMoNbTaTiVZr EE-HEA (No. 17) of a single bcc phase exhibiting $S_m^{mix}/S_m^{ideal} \sim 1$ as the maximum for bcc-EE-HEAs in Fig. 2 The analysis above for bcc phase in Table 3 was also performed for liquid phase of Ni–Ti, Fe–Ti and Mo–Ni sub-binary alloy systems obtained by approximating G_m^{mix}. The results for liquid phases are summarized in Table 4 shows that these alloys in a liquid phase exhibit positive T dependence of $\Omega_{i-j}(T)$, resulting in decreasing S_m^{mix}/R from its ideal value of $\ln 2 = 0.693$.

A similar analysis was performed for all the sub-binary systems of the CoCrFeMnNi EE-HEA as shown in Fig. 4. Features of the sub-binary systems of the CoCrFeMnNi EE-HEA were that the values of the S_m^{mix}/R at each equiatomic composition (at $x_B = 0.5$) are smaller than $S_m^{mix}/R = \ln 2$ in only three sub-binary systems of Fe–Ni, Fe–Mn and Cr–Mn. This would considerably contribute to increase the S_m^{mix}/R of the fcc-CoCrFeMnNi HEA (No. 3) by 9% than $\ln N$ as demonstrated in Table 1. In general, T dependence of $\Omega_{i-j}(T)$ of the EE-HEAs necessarily became averaged in magnitude as shown in eqs. (8) due to alloying within the maximum and minimum tendencies of T dependences of $\Omega_{i-j}(T)$'s of the sub-binary systems. This averaging can be confirmed in the second line of eqs. (9) in a process of summation for $j \neq i$

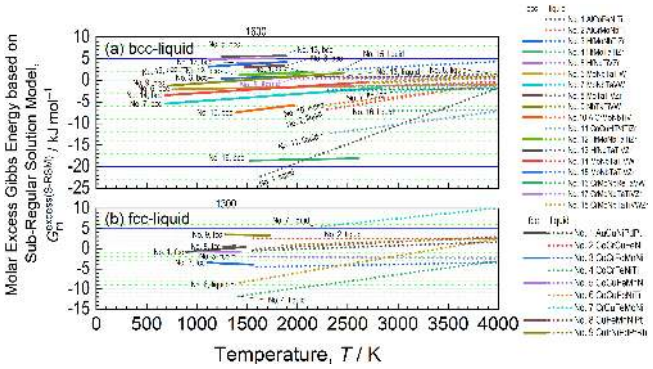

Fig. 5 $G_m^{excess(S-RSM)}$–T chart based on a sub-regular solution model of (a) bcc- and (b) fcc-EE-HEAs and their liquid phases calculated with Thermo-Calc. The positive or negative sign of the slope of the plots indicates the decrease or increase, respectively, in S_m^{mix}/R from its ideal value of $S_m^{mix}/R = \ln N$. $G_m^{excess(S-RSM)}$–T chart can be converted to G_m^{mix}–T chart by subtracting $TS_m^{ideal} = RT\ln N$ due to $G_m^{mix} = G_m^{excess(S-RSM)} - TS_m^{ideal}$ where G_m^{mix}–T chart directly express S_m^{mix} by the slopes of the plots.

and i. Figure 4 differs from Fig. 3 in that most of S_m^{mix}/R's excepting for Cr–Fe, Co–Ni, Fe–Mn sub-binary systems in Fig. 4 exhibit asymmetric profiles against $x_B = 0.5$. These asymmetric characteristics of the plots never affect the present approximation for EE-HEAs that hold exact equiatomicity. However, they might affect the applicability of the present approximation technique to near-equiatomic-(NE-) HEAs. These asymmetric characteristics could be dealt with a sub-regular solution model where $\Omega_{i-j}(T)$ in eqs. (6) allows v from odd numbers.

3.5 Advantageous features of $G_m^{excess(S-RSM)}$–T and G_m^{mix}–T charts

The above tendencies of S_m^{mix}/R were investigated for all the bcc- and fcc-EE-HEAs in a form of $G_m^{excess(S-RSM)}$–T chart[37] based on the sub-regular solution model. Figure 5 shows that most of the plots, excepting for three fcc-EE-HEAs of CoCrFeMnNi (No. 3), CoCuFeMnNi (No. 5) and CuIrNiPdPtRh (No. 8) alloys in each single fcc phase in Fig. 5(b), can be approximated as linear functions. This suggests that most of the EE-HEAs possess a simple linear T dependence of $\Omega_{i-j}(T)$, indicating the presence of $b^{(0)}$ and absence of $c^{(0)}$ term as shown in eqs. (10) and Tables 3 and 4. The $G_m^{excess(S-RSM)}$–T chart indicates that the positive or negative sign of the slope of the plots indicates the decrease or increase in S_m^{mix}/R from its ideal value of $S_m^{mix}/R = \ln N$. Figure 5(a) demonstrates that almost all the bcc-EE-HEAs in single bcc and liquid phases (solid and dotted lines, respectively) exhibited positive slopes over a T range of 1300 K (bcc phase) and 4000 K (liquid phase), suggesting $S_m^{mix}/R < \ln N$. Minor exceptions were the CrMoNbTaTiVZr EE-HEA (No. 17) of a single bcc phase and the HfNbTiVZr (No. 5) and HfNbTaTiVZr (No. 13) alloys formed in a liquid phase. These three are plotted almost flat in Fig. 5(a), corresponding to $S_m^{mix}/S_m^{ideal} \sim 1$ in Fig. 2. The AlCoFeNiTi alloy (No. 1) in the liquid state exhibits the largest positive slope in Fig. 5(a), explaining the smallest value of the ratio of $S_m^{mix}/S_m^{ideal} = 0.354$ as shown in Fig. 2. In strong contrast, Fig. 5(b) indicate that some of the fcc-EE-HEAs formed in

an fcc solid solutions over a T range of 1600 K exhibited weak negative slopes, such as CoCrFeMnNi (No. 3) and CoCuFeMnNi (No. 5) and CuIrNiPdPtRh (No. 9) systems. The negative slopes of these three alloys in Fig. 5(b) explained $S_m^{mix}/R > \ln N$. Here, as supplementals, T dependency of $\Omega_{i-j}(T)$ of the fcc-CoCrFeMnNi EE-HEA exhibiting $S_m^{mix}/R > \ln N$ does not agree with an early report[37] where the plots in $G_m^{excess(S\text{-}RSM)}$–$T$ chart indicates the positive slope. This disagreement with the early[37] and the present study would be due to the different databased for the analysis. Further investigation will be performed shortly regarding this difference.

The significance of the present analysis was to focus on the T dependence of $\Omega_{i-j}(T)$. The present results indicate that $S_m^{mix}/R < \ln N$ when T dependence of $\Omega_{i-j}(T) > 0$ and $S_m^{mix}/R > \ln N$ when T dependence of $\Omega_{i-j}(T) < 0$. The above results suggested that selecting binary systems with negative temperature dependence of $\Omega_{i-j}(T)$ efficiently from the database would lead to developing novel super EE-HEAs. This partially takes place in the fcc-CoCrFeMnNi EE-HEA where seven sub-binary systems apart from only the three Fe–Ni, Fe–Mn and Cr–Mn sub-binary systems tended to increase S_m^{mix}/R. This example of fcc-CoCrFeMnNi EE-HEA implies that one could find out truly HEAs that possess considerably high S values than $S_m^{mix}/R = \ln N$ by utilizing the negative T dependence of H^{mix}.

The G_m^{mix}–T chart can be drawn by subtracting $RT\ln N$ due to a relationship of $G_m^{mix} = G_m^{excess} - TS_m^{ideal}$. An advantageous aspect of the G_m^{mix}–T chart is that a fundamental thermodynamic relationships, $G = H - TS$ and $S = -(\partial G/\partial T)_P$ hold between G_m^{mix} and T. The latter relationship helps to evaluate S_m^{mix} directly from the slope of the G_m^{mix}–T chart, which can be regarded as the significant aspect. In contrast, the G_m^{mix}–T chart does not provide the universal trends among the EE-HEAs with different N, such as, $S_m^{mix}/R < \ln N$ when T dependence of $\Omega_{i-j}(T) > 0$ and $S_m^{mix}/R > \ln N$ when T dependence of $\Omega_{i-j}(T) < 0$ from the $G_m^{excess(S\text{-}RSM)}$–$T$ chart. However, the G_m^{mix}–T chart is of great importance in a process of approximating G_m^{mix} and subsequent obtaining coefficients of the v-th order, in particular, $a^{(0)}$, $b^{(0)}$ and $c^{(0)}$ of $L_{EE\text{-}HEA}^{(0)}(T)$ in eqs. (9) for EE-HEAs. For instance, the representative $L_{EE\text{-}HEA}^{(0)}(T)$ of bcc-MoNbTaVW and fcc-CoCrFeMnNi with a single solid phase summarized in Table 5 shows that the sign of Judgment Factor, $(b^{(0)} + R\ln N) + c^{(0)}(\ln T + 1)$, whether positive or negative determines $R\ln N - S_m^{mix} > 0$ ($S_m^{mix} < R\ln N$) or $R\ln N - S_m^{mix} < 0$ ($S_m^{mix}/R > R\ln N$), respectively. The wide applicability of $G_m^{excess(S\text{-}RSM)}$–$T$ chart necessarily results from G_m^{mix}–T charts where the latter chart has a process of calculating G_m^{mix} by eqs. (5) and subsequent fitting as eqs. (6) and (7) to obtain coefficients. It is expected that researches of EE- and NE-HEAs will proceed by utilizing advantageous aspects and by compensating for each disadvantageous point between $G_m^{excess(S\text{-}RSM)}$–$T$ and G_m^{mix}–T charts.

3.6 Estimation of ranges of S_m^{mix}/R and S_m^{mix}/S_m^{ideal} of EE-HEAs

In a framework of the sub-regular solution model, the ranges of S_m^{mix}/R and S_m^{mix}/S_m^{ideal} of the EE-HEAs were estimated by plotting the alloys in an X-Y chart with H_m^{excess} and S_m^{excess}, respectively, which consist of $H_m^{excess(S\text{-}RSM)}$ in a part of eqs. (11). Figure 6 depict the plots of the EE-HEAs for $X = a^{(0)} - c^{(0)}T$ and $Y = \{b^{(0)} + R\ln 2 + c^{(0)}(\ln T + 1)\}/(\ln N/\ln 2)$ as well as two additional perpendicular axes (Y_1 and Y_2) for comparison. The $\ln N/\ln 2$ in Y-axis was the conversion factor to adjust the magnitude of the quantities of the N-component EE-HEAs to that of binary alloys ($N = 2$). In Fig. 6, the ideal solution is demonstrated by $Y = 0$, $Y_1 = \ln N$, and $Y_2 = 1$. The analysis with Fig. 6 revealed that

Table 5 Coefficients ($a^{(0)}$, $b^{(0)}$ and $c^{(0)}$) of the 0th order of the interaction parameter, $L_{EE\text{-}HEA}^{(0)}(T)$, of bcc-MoNbTaVW and fcc-CoCrFeMnNi a single solid phase. The coefficients were obtained by approximating G_m^{mix} up to T term or $T\ln T$ term for the latter cases from eqs. (9) as $H_{m,EE\text{-}HEA}^{mix} = L_{EE\text{-}HEA}^{(0)}(T) = a^{(0)} + b^{(0)}T + c^{(0)}T\ln T$ where S_m^{mix}/R was able to be computed as $-b^{(0)}/R$ for the former and $-\{b^{(0)} + c^{(0)}(\ln T + 1)\}/R$ for the latter EE-HEA. The magnitude of S_m^{mix} smaller or larger than $R\ln N$ has a relationship to the judgment factor (JF), $R\ln N - S_m^{mix} = (b^{(0)} + R\ln N) + c^{(0)}(\ln T + 1)$, which corresponds with the slope of the $G_m^{excess(S\text{-}RSM)}$–$T$ chart by its sign of whether positive or negative, resulting in $R\ln N - S_m^{mix} > 0$ ($S_m^{mix} < R\ln N$) or $R\ln N - S_m^{mix} < 0$ ($S_m^{mix}/R > R\ln N$), respectively.

Phase-Alloy No.	EE-HEA	$a^{(0)}$ / J mol^{-1}	$(b^{(0)}+R\ln N)$ / J mol^{-1} K^{-1}	$c^{(0)}$ / J mol^{-1}	Judgment Factor: $(b^{(0)}+R\ln N)+c^{(0)}(\ln T+1)$ / J mol^{-1}
bcc-No.7	MoNbTaVW	−6584.6	1.7198	0	1.7198
bcc-No.17	CrMoNbTaTiVZr	4217.1	−0.0669	0	−0.0669
fcc-No. 1	AuCuNiPdPt	−2686.8	2.1069	0	2.1069
fcc-No. 3	CoCrFeMnNi at 1300 K	1354.3	−23.4874	2.7340	−1.1502
fcc-No. 5	CoCuFeMnNi at 1300 K	2436.2	−19.7224	2.4095	−0.0361
fcc-No. 8	CuFeMnNiPt at 1300 K	−1853.3	7.5169	−0.7877	1.0811
fcc-No. 9	CuIrNiPdPtRh	4116.8	−0.4717	0	−0.4717

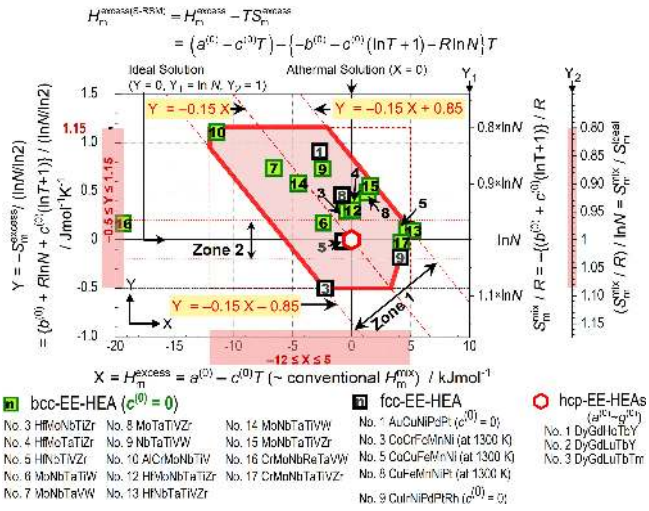

Fig. 6 Relationships between $X = H_m^{excess}$ and $Y = -S_m^{excess}/(\ln N/\ln 2)$ where H_m^{excess} and S_m^{excess} consist of $H_m^{excess(S\text{-}RSM)}$ in a framework of the sub-regular solution model. The factor of $\ln N/\ln 2$ is a denominator for the N-component EE-HEAs to convert their magnitude to those of binary alloy ($N = 2$). The X-Y chart is accompanied by additional perpendicular axes (Y_1 and Y_2) with reverse direction to Y-axis. The values of Y's were calculated after determining T for the fcc-EE-HEAs with Nos. 3, 5 and 8 because of the presence of $c^{(0)}$ term. Besides, the values of the EE-HEAs with hcp structure needed to use coefficients up to the $g^{(0)}$ term by referring to eqs. (A.2) and (A.3) in the Appendix because of a rather small increase in G_m^{mix} at a low-temperature range of $T \le 1000$ K. However, the magnitude of the X of the EE-HEAs with hcp structure can be evaluated to be ~0 in the units of kJ mol^{-1} and that of the $Y \sim 0$ Jmol^{-1}K^{-1}.

the EE-HEAs tended to be plotted along a zone (Zone 1) that distributes through the second and fourth quadrants of Fig. 6 in the X-Y axes. The Zone 1 consists of a direct proportional approximation function of $Y = -0.15X$ drawn with a dash-dotted line and two parallel lines of different intersections of ± 0.85.

The ranges of S_m^{mix}/R and S_m^{mix}/S_m^{ideal} of EE-HEAs were estimated from conventional H_m^{mix} in X-axis. Figure 6 demonstrates that all the EE-HEAs exhibited H^{mix} in a range of $-20 \leq H^{mix}/\mathrm{kJ\,mol^{-1}} \leq 5$, which exactly agreed with the data by Zhang *et al.*[38] and almost corresponded with $-22 \leq H^{mix}/\mathrm{kJ\,mol^{-1}} \leq 7$ by Guo and Liu.[39] On the other hand, the present H^{mix} in Fig. 6 in a range of $-12 \leq H^{mix}/\mathrm{kJ\,mol^{-1}} \leq 5$ by excepting the bcc-HEA with No. 16 roughly agreed with $-11.6 \leq H^{mix}/\mathrm{kJ\,mol^{-1}} \leq 3.2$ reported by Guo *et al.*[40] In this exceptional case of $-12 \leq H^{mix}/\mathrm{kJ\,mol^{-1}} \leq 5$, a rectangular area was formed with $-0.5 \leq Y \leq 1.15$ from approximate maximum and minimum values of S_m^{mix}/S_m^{ideal}, which were given from the fcc-EE-HEAs with Nos. 3 and bcc-EE-HEAs with Nos. 10, respectively. Then, considering the overlap between the rectangular and Zone 1 led to the truncated polygon hatched in Fig. 6, which includes almost all the plots of the EE-HEAs exception for the bcc-EE-HEA with No. 16 (CrMoNbReTaVW). Thus, it was found that Zone 1 worked effectively to screening the EE-HEAs with the support of the limits of conventional H_m^{mix} of the EE-HEAs.

The exceptional plot of the bcc-EE-HEA with No. 16 in Fig. 6 was included in another zone (Zone 2) that contains candidates of EE-HEA as well as X-axis with $Y = 0$, $Y_1 = \ln N$, and $Y_2 = 1$ as defined by the ideal solid solution. Although the range (width) of Zone 2 is unclear, Zone 2 given in Fig. 6 also contains the bcc-EE-HEA with Nos. 5, 6, 13, and 17, the fcc-EE-HEA with Nos. 5 and 9 as well as hcp-EE-HEAs with Nos. 1–3 in addition to bcc-EE-HEA with No. 16. Thus, Zone 2 based on the characteristics of the ideal- and near-ideal solid solutions is significant as well as Zone 1 for screening the plots of EE-HEAs.

The results above suggested that the EE-HEAs would possess S_m^{mix}/R and S_m^{mix}/S_m^{ideal} in an approximate range of 20% lower to 10% greater than the ideal solid solutions. It is expected that novel EE-HEAs can be developed by utilizing the above results from Fig. 6.

4. Conclusions

Exact equiatomic high-entropy alloys (EE-HEAs) with N-component ($N \geq 5$) formed into a single-phase experimentally confirmed were analyzed thermodynamically for such representative alloys as bcc-NbMoTaVW, fcc-CoCrFeMnNi, and hcp-heavy lanthanides with and without Y. The analysis revealed that mixing entropy (S^{mix}) does not correspond with either ideal entropy (S^{ideal}) nor configuration entropy (S^{config}) in case of presenting temperature dependence of $\Omega_{i-j}(T)$ of i-j atomic pairs in mixing enthalpy (H^{mix}) of a sub-binary system. The calculations with Thermo-Calc using TCHEA4 as well as SSOL5 database indicate that bcc-MoNbTaVW and NbTaTiVW EE-HEAs exhibited S^{mix} normalized with gas constant (R), S^{mix}/R, smaller by 13% to $S^{ideal}/R = \ln N$. In contrast, CoCrFeMnNi, CoCuFeMnNi fcc-EE-HEAs exhibited greater S^{mix}/R than $\ln N$. These different tendencies can be explained by the T dependence of $\Omega_{i-j}(T)$ in H^{mix}. As an exceptional case, the hcp-EE-HEAs comprising heavy lanthanides mainly from athermal solutions behave as ideal solutions. The $G_m^{excess(S\text{-}RSM)}$–$T$ chart from the sub-regular solution model declared that the positive or negative signs of the slope of plots directly represent $S^{mix}/R < \ln N$ or $S^{mix}/R > \ln N$, respectively. The present results from the sub-regular solution model have clarified that EE-HEAs do not always exhibit $S^{mix}/R = \ln N$ in case of the presence of T dependence of $\Omega_{i-j}(T)$ in H^{mix} that affects S^{mix}. The present results with the help of H^{mix} analysis revealed that the EE-HEAs would possess S^{mix}/R approximately 20% smaller or 10% greater than S^{ideal}/R as their minimum or maximum limits.

Appendix

The following describes a case when G_m^{mix} is necessary to describe with the succeeding terms to $cT\ln T$ in eqs. (5), such as eqs. (A.1). According to unary SGTE (Scientific Group Thermodata Europe) database,[36] ${}^0G_m^{\alpha} - {}^0H_m^{298.15}$ could be described with $T\ln T$ and polynomials of T^n ($0 \leq n \leq 4$ or 7), T^{-m}, ($m = 1$ or 9) where ${}^0H_m^{298.15}$ is an enthalpy at 298.15 K from standard element reference stage. Below, G_m^{mix} was supposed to be described with $T\ln T$ and polynomials as eqs. (A.1).

$$G_m^{mix} = a + bT + cT\ln T + dT^2 + eT^3 + fT^{-1} + gT^4 + hT^7 + iT^{-9} + \quad \text{(A.1)}$$

Applying $G = H - TS$ and $S = -(\partial G/\partial T)_P$ to eqs. (A.1) yields eqs. (A.2) and (A.3).

$$S_m^{mix} = -b - c(\ln T + 1) - 2dT - 3eT^2 + fT^{-2} - 4gT^3 - 7hT^6 + 9iT^{-10} \quad \text{(A.2)}$$

$$H_m^{mix} = a - cT - dT^2 - 2eT^3 + 2fT^{-1} - 3gT^4 - 6hT^7 + 10iT^{-9} \quad \text{(A.3)}$$

In case of necessity of using the succeeding terms to $cT\ln T$ in eqs. (5), eqs. (A.1) to (A.3) could be used for analysis. In this case, a criteria to judge (Judgement Factor) whether the system of interest has S^{mix}/R greater or smaller than $\ln N$ is expressed as eqs. (A.4)/R instead of $\{-b^{(0)} - c^{(0)}(\ln T + 1)\}/R$ in Table 3.

$$\{-b^{(0)} - c^{(0)}(\ln T + 1) - 2d^{(0)}T - 3e^{(0)}T^2 + f^{(0)}T^{-2} - 4g^{(0)}T^3 - 7h^{(0)}T^6 + 9i^{(0)}T^{-10}\} \quad \text{(A.4)}$$

In practice, eqs. (A.1) and subsequent eqs. (A.2) to (A.4) do not necessary in approximating G_m^{mix} instead of eqs. (5), since even a complicated formulation of eqs. (A.1) could be divided into simple formulations, such as eqs. (5) by selecting appropriate temperature ranges. Equations (A.2) and (A.3) demonstrate that coefficients of a and b in eqs. (5) as well as relevant $a^{(0)}$ and $b^{(0)}$ from 0-th order approximation in eq. (7) are inherent coefficients to H_m^{mix} and S_m^{mix}, respectively. On the other hand, coefficients c and $c^{(0)}$ in eqs. (5) and subsequent coefficients, d to i in eqs. (A.2) and (A.3) and relevant $d^{(0)}$ to $i^{(0)}$ in the 0-th order approximation, have a characteristic of affecting both H_m^{mix} and S_m^{mix}.

Acknowledgment

This work was supported by JSPS KAKENHI Grant Number JP17H03375.

REFERENCES

1) B.S. Murty, J.-W. Yeh and S. Ranganathan: *High-Entropy Alloys*, (Butterworth-Heinemann, London, U.K., 2014).
2) M.C. Gao: *High-Entropy Alloys: Fundamentals and Applications*, (Springer, Berlin, 2016) pp. xiii, 516 p.
3) B.S. Murty, J.-W. Yeh, S. Ranganathan and P.P. Bhattacherjee: *High Entropy Alloys*, (Elsevier, Amsterdam, 2019) pp. xxiii, 363.
4) J.W. Yeh, S.K. Chen, S.J. Lin, J.Y. Gan, T.S. Chin, T.T. Shun, C.H. Tsau and S.Y. Chang: Adv. Eng. Mater. **6** (2004) 299–303.
5) B. Cantor, I.T.H. Chang, P. Knight and A.J.B. Vincent: Mater. Sci. Eng. A **375–377** (2004) 213–218.
6) T. Abe: *Thermodynamic Calculation and Analysis Based on CALPHAD Method*, (Uchida Rokakuho, Tokyo, 2019) pp. 48–49 (in Japanese).
7) "Thermo-Calc Version 2020a (Thermo-Calc Documentation Set)", https://www.thermocalc.com/support/documentation/, (accessed 2020-05-21).
8) N.N. Guo, L. Wang, L.S. Luo, X.Z. Li, Y.Q. Su, J.J. Guo and H.Z. Fu: Mater. Des. **81** (2015) 87–94.
9) O.N. Senkov, G.B. Wilks, D.B. Miracle, C.P. Chuang and P.K. Liaw: Intermetallics **18** (2010) 1758–1765.
10) O.N. Senkov, G.B. Wilks, J.M. Scott and D.B. Miracle: Intermetallics **19** (2011) 698–706.
11) Z.D. Han, N. Chen, S.F. Zhao, L.W. Fan, G.N. Yang, Y. Shao and K.F. Yao: Intermetallics **84** (2017) 153–157.
12) B.L. Zhang, Y. Mu, M.C. Gao, W.J. Meng and S.M. Guo: MRS Commun. **7** (2017) 78–83.
13) H. Chen, A. Kauffmann, B. Gorr, D. Schliephake, C. Seemuller, J.N. Wagner, H.J. Christ and M. Heilmaier: J. Alloy. Compd. **661** (2016) 206–215.
14) C.C. Juan, M.H. Tsai, C.W. Tsai, C.M. Lin, W.R. Wang, C.C. Yang, S.K. Chen, S.J. Lin and J.W. Yeh: Intermetallics **62** (2015) 76–83.
15) O.V. Sobol', A.A. Andreev, V.F. Gorban', N.A. Krapivka, V.A. Stolbovoi, I.V. Serdyuk and V.E. Fil'chikov: Tech. Phys. Lett. **38** (2012) 616–619.
16) D. Karlsson, G. Ek, J. Cedervall, C. Zlotea, K.T. Moller, T.C. Hansen, J. Bednarcik, M. Paskevicius, M.H. Sorby, T.R. Jensen, U. Jansson and M. Sahlberg: Inorg. Chem. **57** (2018) 2103–2110.
17) Y.K. Mu, H.X. Liu, Y.H. Liu, X.W. Zhang, Y.H. Jiang and T. Dong: J. Alloy. Compd. **714** (2017) 668–680.
18) H.W. Yao, J.W. Qiao, M.C. Gao, J.A. Hawk, S.G. Ma, H.F. Zhou and Y. Zhang: Mater. Sci. Eng. A **674** (2016) 203–211.
19) S.A. Firstov, T.G. Rogul', N.A. Krapivka, S.S. Ponomarev, V.N. Tkach, V.V. Kovylyaev, V.F. Gorban' and M.V. Karpets: Russ. Metall. **2014** (2014) 285–292.
20) A. Takeuchi, K. Amiya, T. Wada and K. Yubuta: Mater. Trans. **57** (2016) 1197–1201.
21) M.C. Gao, B. Zhang, S. Yang and S.M. Guo: Metall. Mater. Trans. A **47** (2016) 3333–3345.
22) J.H. Kim, K.R. Lim, J.W. Won, Y.S. Na and H.S. Kim: Mater. Sci. Eng. A **712** (2018) 108–113.
23) M.J. Jang, S. Praveen, H.J. Sung, J.W. Bae, J. Moon and H.S. Kim: J. Alloy. Compd. **730** (2018) 242–248.
24) K. Ichii, M. Koyama, C.C. Tasan and K. Tsuzaki: Scr. Mater. **150** (2018) 74–77.
25) J. Freudenberger, D. Rafaja, D. Geissler, L. Giebeler, C. Ullrich, A. Kauffmann, M. Heilmaier and K. Nielsch: Metals **7** (2017) 135.
26) G. Qin, S. Wang, R.R. Chen, X. Gong, L. Wang, Y.Q. Su, J.J. Guo and H.Z. Fu: J. Mater. Sci. Technol. **34** (2018) 365–369.
27) K.B. Zhang, Z.Y. Fu, J.Y. Zhang, W.M. Wang, H. Wang, Y.C. Wang, Q.J. Zhang and J. Shi: Mater. Sci. Eng. A **508** (2009) 214–219.
28) Tazuddin, N.P. Gurao and K. Biswas: J. Alloy. Compd. **697** (2017) 434–442.
29) X. Wang, H. Xie, L. Jia and Z. Lu: 13th International Symposium on Eco-Materials Processing and Design, ISEPD 2012, (Guilin, 2012) pp. 335–338.
30) C. Li, J.C. Li, M. Zhao and Q. Jiang: J. Alloy. Compd. **475** (2009) 752–757.
31) A. Takeuchi, T. Wada and Y. Zhang: Intermetallics **82** (2017) 107–115.
32) S.W. Sohn, Y.H. Liu, J.B. Liu, P. Gong, S. Prades-Rodel, A. Blatter, B.E. Scanley, C.C. Broadbridge and J. Schroers: Scr. Mater. **126** (2017) 29–32.
33) J. Lužnik, P. Koželj, S. Vrtnik, A. Jelen, Z. Jagličić, A. Meden, M. Feuerbacher and J. Dolinšek: Phys. Rev. B **92** (2015) 224201.
34) A. Takeuchi, K. Amiya, T. Wada, K. Yubuta and W. Zhang: JOM **66** (2014) 1984–1992.
35) Y.J. Zhao, J.W. Qiao, S.G. Ma, M.C. Gao, H.J. Yang, M.W. Chen and Y. Zhang: Mater. Des. **96** (2016) 10–15.
36) "Version 5.0 of Unary database - 2 June 2009", Scientific Group Thermodata Europe, http://www.crct.polymtl.ca/sgte/unary50.tdb, (accessed 2020-03-11).
37) T. Abe: Mater. Trans. **61** (2020) 610–615.
38) Y. Zhang, Y.J. Zhou, J.P. Lin, G.L. Chen and P.K. Liaw: Adv. Eng. Mater. **10** (2008) 534–538.
39) S. Guo and C.T. Liu: Prog. Nat. Sci.-Mater. **21** (2011) 433–446.
40) S. Guo, Q. Hu, C. Ng and C.T. Liu: Intermetallics **41** (2013) 96–103.